Stable and Fluid Multilayer Phospholipid–Silica Thin Films: Mimicking Active Multi-lamellar Biological Assemblies

Gautam Gupta,[†,‡] Srinivas Iyer,[§] Kara Leasure,[§] Nicole Virdone,[⊥,¶] Andrew M. Dattelbaum,[‡] Plamen B. Atanassov,[†] and Gabriel P. López[†,⊥,¶,*]

[†]Center for Biomedical Engineering, Department of Chemical and Nuclear Engineering, University of New Mexico, Albuquerque, New Mexico 87131, United States, [‡]Center for Integrated Nanotechnologies, MS K771, and [§]Bioenergy and Biome Sciences Group, MS M888, Los Alamos National Laboratory, Los Alamos, New Mexico 87545, United States, and [⊥]Department of Mechanical Engineering & Materials Science, [¶]NSF Research Triangle Materials Research Science and Engineering Center, Department of Biomedical Engineering, Duke University, Durham, North Carolina 27708, United States

ABSTRACT Phospholipid-based nanomaterials are of interest in several applications including drug delivery, sensing, energy harvesting, and as model systems in basic research. However, a general challenge in creating functional hybrid biomaterials from phospholipid assemblies is their fragility, instability in air, insolubility in water, and the difficulty of integrating them into useful composites that retain or enhance the properties of interest, therefore limiting there use in integrated devices. We document the synthesis and characterization of highly ordered and stable phospholipid–silica thin films that resemble multilamellar architectures present in nature such as the myelin sheath. We have used a near room temperature chemical vapor deposition method to synthesize these robust functional materials. Highly ordered lipid films are exposed to vapors of silica precursor resulting in the formation of nanostructured hybrid assemblies. This process is simple, scalable, and offers advantages such as exclusion of ethanol and no (or minimal) need for exposure to mineral acids, which are generally required in conventional sol–gel synthesis strategies. The structure of the phospholipid–silica assemblies can be tuned to either lamellar or hexagonal organization depending on the synthesis conditions. The phospholipid–silica films exhibit long-term structural stability in air as well as when placed in aqueous solutions and maintain their fluidity under aqueous or humid conditions. This platform provides a model for robust implementation of phospholipid multilayers and a means toward future applications of functional phospholipid supramolecular assemblies in device integration.

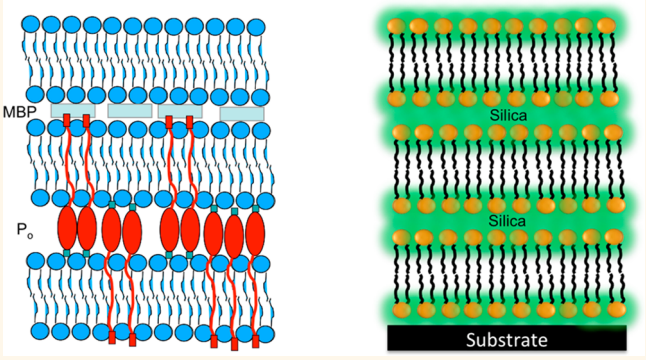

KEYWORDS: myelin · multilamellar · hybrid phospholipid silica assemblies · fluid membranes · air-stable lipid assemblies

Phospholipids are the primary components of biological membranes that act in part as physicochemical barriers to compartmentalize cells and organelles.[1] These membranes are dynamic and fluid in nature, incorporating transmembrane proteins that perform critical functions including solute transport, signal transduction, and ATP synthesis.[2] The importance of biological cellular membranes has inspired an enormous body of research using various model systems that mimic, to various extents, the behavior and properties of native biological membranes in controlled laboratory environments. These include black lipid membranes,[3] liposomes,[4] supported lipid bilayers,[5] and tethered bilayer lipid membranes.[6] Translation of these models to functional lipid-based biomaterials for sensing, separation and energy harvesting devices has been challenging because model lipid systems are fragile, lacking long-term stability in aqueous solutions, and rapidly degraded in air and at air–water interfaces.[7,8]

In addition to single lipid bilayers, complex multilamellar structures play a critical role in native biological systems. For example, multilamellar lipid bilayer structures are found within

* Address correspondence to gabriel.lopez@duke.edu.

Received for review March 5, 2013 and accepted May 24, 2013.

Published online May 24, 2013
10.1021/nn401123p

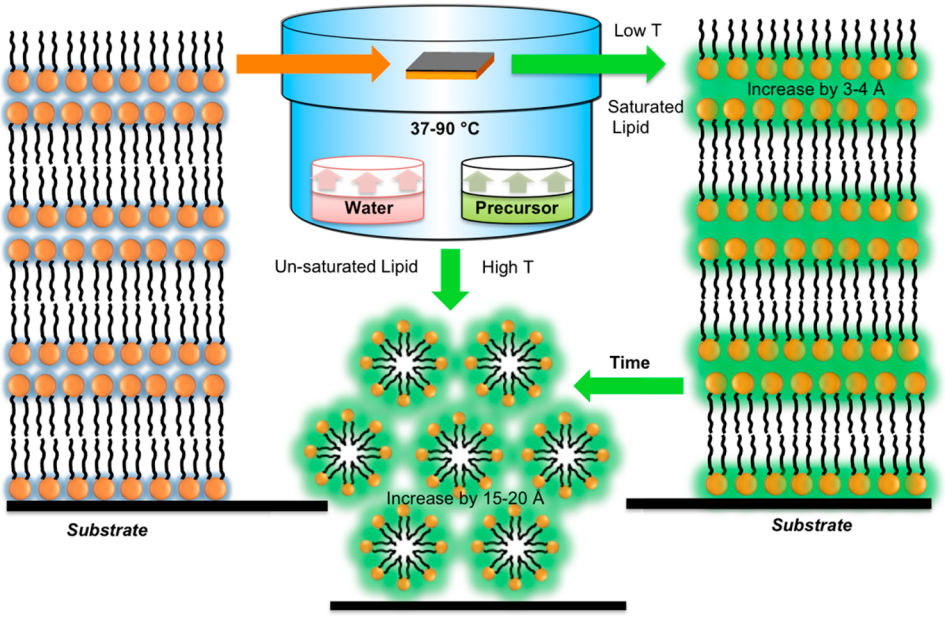

Figure 1. Schematic of the CVD process used to prepare silica encapsulated multilamellar lipid assemblies. Spin-coated multilamellar lipid stacks (left) are exposed to vapors of a silica precursor (TEOS or TMOS) and water. Silica forms selectively between the lipid head groups of the lamellar lipid assemblies. An increase in synthesis temperature, use of unsaturated lipid, and long exposure times result in the formation of hexagonal phases.

the nervous system (*e.g.*, in the myelin sheath)[9,10] and lung surfactants.[11] Despite the importance of multilamellar assemblies in biological systems, there is a dearth of useful multilamellar lipid model systems, chiefly due to their loss of structural integrity upon exposure to aqueous conditions. Ordered multilamellar phospholipid structures prepared by spin- or drop-casting on solid supports have been studied to obtain detailed structural information of lipids and understanding of the influence of hydration on the lipid assembly, for example, by nuclear magnetic resonance,[12] X-ray diffraction,[13] X-ray reflectivity,[14] and neutron reflectivity,[15,16] but functional characterization has been problematic due to the rapid delamination and disruption of multilamellar lipid films upon hydration.[17,18] Thus, new strategies are needed to prepare multilamellar assemblies with improved stability, especially in aqueous conditions.

Sol–gel techniques have been used to synthesize functional biomaterials[19–23] and structured mesoporous silica materials using a variety of sacrificial templates (including biomolecular assemblies).[24–29] Despite the success of these techniques, the acids and alcohols used in typical sol–gel processes precludes their use in encapsulation of fragile bioassemblies.[20,30] Recently, we described a sol–gel synthesis methodology based on chemical vapor deposition into liquids, which generates minimal alcohol and can be performed at neutral pH. This technique stabilizes various nano- and microscale bioassemblies, including liposomes, enzymes, microorganisms,[21,31] and surfactant-wrapped carbon nanotubes.[32,33]

Here, we apply a similar technique to synthesize hybrid assemblies of lipids and silica, which may serve as either (i) effective model systems for studying naturally occurring multilamellar nanoscale assemblies such as myelin, or (ii) as components of sensing and energy harvesting, or other devices. In this approach, a highly ordered assembly is prepared by spin-coating lipids onto a substrate (*e.g.*, a silicon wafer) and then exposing the lipids to vapors of an alkyl silicate precursor at a desired temperature. The synthesis conditions can be precisely controlled to achieve either lamellar or hexagonally ordered structures, with thicknesses from 10 to 200 nm. By controlling the thickness of the lipid–silica assemblies, it should be possible to tune these stable, ultrathin films to exhibit varying resistance to mass transport. The nanoscale multilamellar thin films remain intact and can maintain fluidity when placed in hydrated environments. To the best of our knowledge, this is the first report of a hybrid and highly ordered phospholipid-based multilamellar assembly that maintains its structure and fluid functionality upon incorporation into a synthetic inorganic matrix. This technique will lay a foundation for future applications of artificial membranes in a variety of potential applications including biosensing, separations, high throughput drug discovery, and biophysical/biochemical studies.[7,34,35]

RESULTS AND DISCUSSION

Figure 1 schematically depicts formation of the lipid–silica nanoscale assemblies and Supporting Information, Figure SI 1 shows the structure of the lipids used in the study. Briefly, a solution of dimyristoyl phosphatidylcholine (DMPC, a saturated phospholipid) in chloroform (10 mg/mL) was spin-coated onto a silicon substrate at 3000 rpm to spontaneously form a multilamellar lipid assembly. X-ray diffraction data showing the presence of

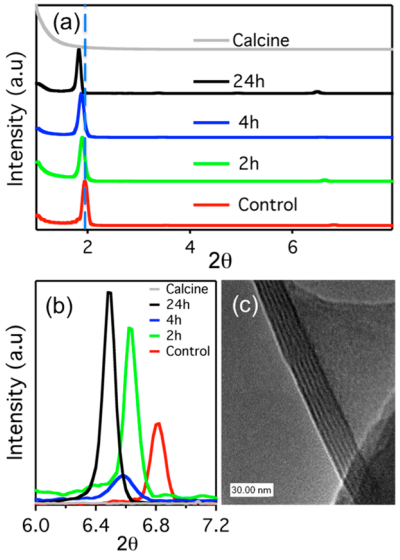

Figure 2. X-ray diffraction patterns and TEM image of lamellar lipid DMPC-silica ultrathin films on silicon wafers synthesized at 60 °C. (a) XRD patterns of lamellar DMPC lipid before exposure, after exposure (2 h, 4 h, 24 h), and after calcination; (b) 4th order diffraction peaks of similar samples; (c) TEM image of lamellar lipid silica assembly (6 layers). The dotted line in Figure 2a indicates the peak position for the spin-coated lipid control sample (control).

(001), (002), (003), and (004) peaks (Figure 2) indicates that the lipid assemblies were highly ordered. The repeat distance (*d*-spacing) was 51.8 Å for pure spin-coated DMPC films. Typically at 10 mg/mL, spinning at 3000 rpm results in a membrane thickness of ~100 nm as confirmed using ellipsometry. These assemblies were then exposed to vapors of a volatile silica precursor, tetraethyl orthosilicate (TEOS), at well above the lipids' gel-fluid transition temperature to allow precursor penetration and ultimately the formation of silica. Typically, this chemical vapor deposition (CVD) process was performed at 60 °C, while the gel transition temperature of DMPC is 23 °C. Hydrochloric acid (0.1 N, aq.) was also included in a separate vial in the vapor chamber to promote efficient hydrolysis of the TEOS vapors. As seen in Figure 2, long-range order of the multilamellar lipid assemblies is maintained after silica deposition, as indicated by the clearly visible fourth order diffraction peaks. After exposure to TEOS for 24 h, the *d*-spacing increased from 51.8 Å to 55 Å (see Figure 5 for intermediate values).

A similar increase in *d*-spacing after silica deposition was observed for numerous hybrid DMPC samples synthesized by exposure to TEOS at 60 °C for 4 or more hours, indicating the precise, self-limiting nature of this synthesis approach. XRD patterns collected at various time intervals suggest the incorporation of silica occurs over a period of 4 h, after which there is no further incorporation (4 and 24 h have similar *d*-spacing). (Figure 2, Figure 5). This may be due to the condensation of silica species between lipid layers that strengthens the silica network, thus preventing further penetration of silica precursor. TEM images of a multilamellar lipid–silica assembly cross-section (Figure 2c) clearly show alternating layers of silica and lipids. The contrast in the image is due to alternating layers of silica (higher electron density) and hydrocarbon chains of lipid molecules (lower electron density). Data from numerous TEM images, together with the presence of higher order XRD peaks after the exposure to the silica precursor, further indicate the formation of highly ordered lamellar structures. The formation of lamellar structures under these conditions was confirmed by grazing incidence small-angle X-ray scattering (data not shown). To further indicate the lamellar structure, we subjected the hybrid assemblies to calcination at 400 °C for 4 h, after which none of the diffraction peaks are observed in the XRD pattern; this suggests the collapse of the lamellar structure upon removal of the organic moieties.

From these data, we propose that this hybrid film synthesis involves two steps: (a) penetration of alkyl silicate precursors (possibly at least partially hydrolyzed) into multilamellar stacks and (b) condensation of silica precursors within the hydrophilic region between lipid head groups; this results in an alternating lipid–silica multilamellar assembly. These assemblies are stable in air and do not delaminate under aqueous conditions, which is a necessary property for numerous membrane-based devices. These films do develop macroscopic cracks in the presence of high humidity (100%) or upon immersion in water, however, which is likely due to condensation of silica at the surface causing the stress gradient along the thickness of the film or the fast adsorption of water increasing capillary pressure and causing stress at the surface.

Synthesis conditions were varied in an effort to tailor the silica–lipid hybrid assemblies with a range of properties that might be useful in functional hybrid membranes. We intended to optimize the synthetic process such that (i) the lipid–silica structure may be modified to a desired phase (*e.g.*, lamellar or hexagonal) by altering lipid composition, temperature, or exposure time, (ii) the acid catalyst can be eliminated, making the technique conducive to incorporating sensitive biological materials, (iii) the synthesis temperature can be decreased to lessen dehydration and/or decrease destabilization of other biomolecules, and finally (iv) the hybrid assemblies can maintain lipid fluidity, are crack resistant, and are not prone to delamination.

To illustrate the effect of deposition temperature on assembly structure, we maintained the multilayer formation conditions and increased the temperature of the CVD process to 90 °C. As shown in Figure 3a, these conditions resulted in a substantial increase in the *d* spacing of the assemblies upon exposure to TEOS vapors. For samples exposed to vapors for 2 h, the (100) peak is observed at 73.4 Å before calcination and 62.3 Å after calcination (see Figure 5 for intermediate values). The *d*-spacing remains constant upon exposure for more than 2 h, indicating that the silica condensation and network strengthening observed in the 60 °C samples occurs sooner at high temperatures. To determine the phase

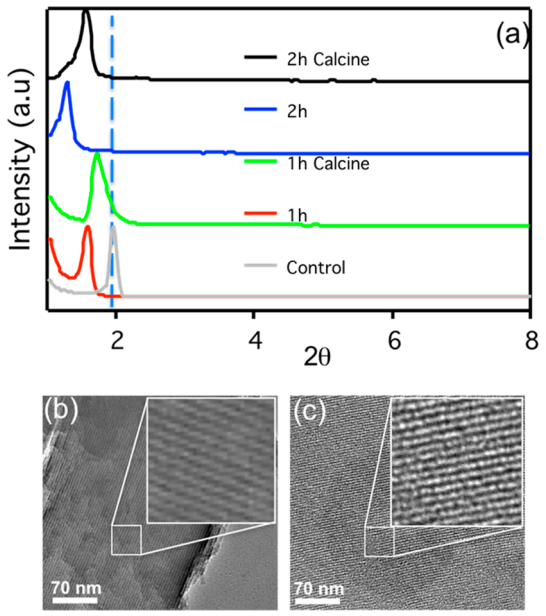

Figure 3. X-ray diffraction and TEM images of hexagonally ordered lipid−silica ultrathin films on silicon wafers synthesized at 90 °C. (a) XRD patterns of DMPC films before and after exposure (1 h, 2 h) and after calcination. TEM image of hexagonal lipid−silica assembly (top view: multiple layer) (b) before calcination and (c) after calcination. The dotted line in panel a indicates the peak position for the spin-coated lipid control sample.

of these hybrid assemblies, we subjected the samples to calcination at 400 °C for 4 h (Figure 3a). The absence of a (110) peak indicates that the hexagonal phase is parallel to the substrate. A decrease in *d* spacing of 11 Å is observed after calcination, which indicates the removal of the template (lipid) and shrinkage of the silica network due to further condensation. This effect is similar to that observed in the synthesis of surfactant templated mesoporous silica materials.[24,25,27,28] Furthermore, TEM micrographs of a sample before and after calcination also indicate the presence of hexagonal assemblies (Figure 3b,c). We also performed grazing-incidence small-angle X-ray scattering (GISAXS) measurements to confirm the transition from lamellar to hexagonal phase as shown in Supporting Information, Figure SI 2 (A-C). XRD is a beneficial tool for providing information on orders parallel to the substrate surface (for example, parallel lipid bilayers); however, order within planes normal to the substrate is more difficult to ascertain. An increase in *d* spacing of 3 Å is observed after TEOS penetration at 60 °C, furthermore a clear indication of hexagonal transformation is obtained at 90 °C. These results indicate that the temperature during synthesis can be adjusted to control the final architecture of the lipid−silica hybrids.

Although both lamellar and hexagonal DMPC-silica hybrid assemblies have highly periodic structures and are air-stable, they possess two properties that may be unfavorable to membrane function: (i) they are prone to cracking and (ii) they are likely to have low phopholipid mobility at room temperature because of the high phase-transition temperature of DMPC. To circumvent these potential issues, we synthesized hybrid assemblies that incorporate lipids with lower phase transition temperatures. Changing the lipid composition had a profound effect on the structure of the final assembly. Egg phosphatidyl choline (egg PC, Supporting Information, Figure SI 1) is a naturally occurring lipid mixture with the same headgroup as DMPC (*i.e.*, should interact similarly with silica), but exhibits a lower phase transition temperature (*i.e.*, is fluid at room temperature) due to the presence of unsaturated fatty acids. We prepared the multilamellar lipid assemblies using a spin coating procedure similar to that described above. The broad first order XRD peak and lack of higher order peaks indicate that the resulting egg PC lipid assemblies were not as ordered as those obtained from DMPC (Supporting Information, Figure SI 3A, Figure 5). The *d*-spacing for these egg PC assemblies was 38 Å; this is lower than expected since the lipids in egg PC mixtures contain longer fatty acid tails than DMPC (Supporting Information, Figure SI 1). These discrepancies may be due to the presence of double bonds, which kink the lipid tails, causing increased fluidity and *d* spacing variance. However, upon exposure to the silica precursor for 1 h at 60 °C, the (001) peak intensity increases and becomes sharper, and higher order peaks (2nd and 3rd order) appear in the XRD pattern (Supporting Information, Figure SI 3A). A decrease in peak widths is observed after exposure to silica precursor (Supporting Information, Table SI 1). This result suggests that the CVD of silica results in hybrid materials that are "more ordered" than the lipid assemblies used to template them.

The first order diffraction peak for samples after 1, 2, and 4 h of exposure to TEOS correspond to *d*-spacings of 48, 66, and 66 Å, respectively. The *d*-spacing measured after a 1 h exposure suggests the formation of a well-arranged lamellar structure, and is consistent with the *d*-spacing expected for an ordered egg PC bilayer. Upon further exposure, a rapid increase in *d* spacing (by 18 Å) is observed, which suggests a phase transformation from lamellar to hexagonal structure. This transition may be possible because the double bonds in the egg PC lipids impart more fluidity that allows the silica framework to reorganize into the hexagonal structure observed. The *d* spacing decreases to 58 Å after calcination due to further condensation of silica species and removal of water and lipid molecules. This data clearly shows that order remained post calcination and thus further suggests the formation of a hexagonal structure. The absence of the (110) reflection suggests that the (100) planes of the hexagonal unit cell are oriented parallel to the substrate surface. These results indicate that we can tune the final assembly to different structural configurations by adjusting the initial lipid composition.

To avoid the complications arising from the mixture of lipids in egg PC, we examined 1,2-dioleoyl-*sn*-glycero-3-phosphocholine (DOPC), which has the same

headgroup as the previously used lipids and a single double bond in each lipid tail. (Supporting Information, Figure SI 1) It is also the most dominant unsaturated lipid (30%) in egg PC. Upon spin coating (and before CVD), these films did not yield higher order diffraction peaks (Supporting Information, Figure SI 3B); however, the *d*-spacing corresponding to the primary peak was 40 Å, slightly higher than that of egg PC (38 Å). Upon exposure to TEOS at 60 °C in the presence of 0.1 N HCl, a similar trend in phase transformation from lamellar to hexagonal as was observed for egg PC after 4 h of vapor exposure. This hexagonal structure also did not collapse upon calcination (Supporting Information, Figure SI 3B).

To reduce the use of acids that may preclude incorporation of biomolecules intolerant of low pH, we conducted a series of exposures at varying acidic concentrations. The XRD patterns of a DMPC-silica assembly synthesized at 60 °C with variable acid concentrations (0−0.1N HCl) are shown in Supporting Information, Figure SI 4A,B (exposed for 4 h). These data show that there is a similar 3 Å increase in *d*-spacing before and after exposure to aqueous solutions regardless of acid concentration, suggesting that the presence of acid has minimal influence on the final structure. However, a decrease in the concentration of water vapor (10% relative humidity (RH)) during TEOS CVD resulted in two closely spaced fourth order diffraction peaks rather than the single peak observed previously (Supporting Information, Figure SI 4A,B). Thus, the presence of water in the CVD chamber is critical for the formation of uniform *d*-spacing lipid−silica films. The two fourth order peaks show an increase in *d* spacing of approximately 1.4 and 2 Å from the lipid-assembly control sample. These data suggest that water vapor is essential for hydrolyzing the silica precursors that penetrate and result in uniform *d* spacing. This argument is strengthened by our observation that, at 50% RH, a uniform increase in *d* spacing is detected even when the aqueous container is not in place. The exact mechanism and sequence of precursor hydrolysis and transport to the bilayer interstices is not clear, however.

We also examined the use of a more volatile precursor, tetramethyl orthosilicate (TMOS), in an effort to achieve lower deposition temperatures. Spin-coated DMPC samples were exposed to vapors of TEOS or TMOS at 37 and 60 °C for 4 h (to ensured a maximum increase in the *d* spacing). The *d* spacing obtained for the multilamellar assembles before, and after exposure to TEOS or TMOS were found to be 50.7, 54.2, and 54.9 Å, respectively. There is a difference of 0.7 Å between the TMOS and TEOS samples, but both maintained lamellar structure. Thus, the overall structural organization is dictated mostly by humidity rather than the choice of silica precursor (Supporting Information, Figure SI 5).

Since fluidity is an important characteristic of naturally occurring lipid membranes, we tested lipid mobility at room temperature after silica deposition. The lipid 1-palmotyl-2-oleoyl phosphatidyl choline (POPC)

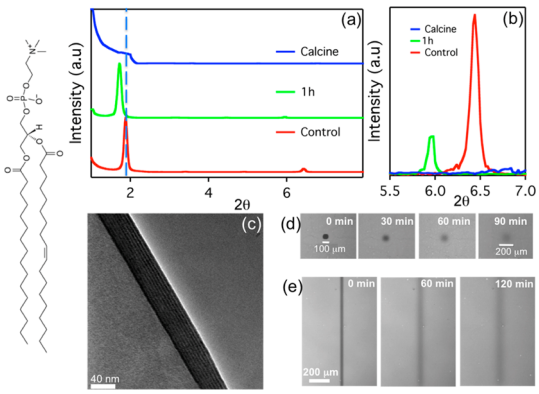

Figure 4. XRD, TEM, and fluorescence images of POPC−silica assemblies prepared on silicon wafers. (a) XRD pattern before and after exposure to silica precursor vapors at 37 °C, and after calcination. (b) XRD patterns of the 4th order diffraction peaks for the samples shown in panel a. (c) TEM image of a POPC−silica assembly before calcination. (d) FRAP of a lamellar POPC−NBD−PE silica film (synthesized at 60 °C) performed in saturated water vapor. (e) FRAP of a lamellar POPC−NBDE−silica film under water (synthesized at 37 °C). The dotted line in panel a was added to reference the (001) peak for all samples relative to the as-prepared spin-coated DMPC lipid assembly.

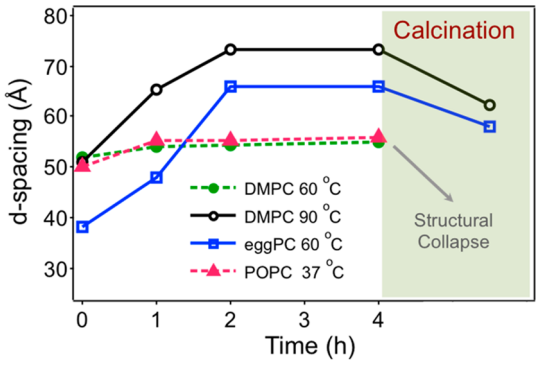

Figure 5. Change in *d*-spacing obtained for various spin-coated lipid films upon exposure to silica precursors. DMPC and egg PC were exposed to TEOS precursor. POPC was exposed to TMOS precursor. Solid lines indicate hexagonal transformation, and dashed lines are examples of lamellar structure.

was used in these studies because it has a phase transition temperature of −2 °C (*i.e.*, is fluid at room temperature) and exhibits the formation of well-ordered lamellar structure upon spin-coating (Figure 4). This lipid has only one double bond in one of its chains, as compared to DOPC, thus leading to a highly ordered structure. To test lipid mobility, we measured fluorescence recovery after photobleaching (FRAP) by incorporating a low concentration of a fluorescently labeled lipid prior to spin coating. We chose a tail-labeled lipid, 1,2-diphytanoyl-*sn*-glycero-3-phosphoethanolamine-*N*-(7-nitro-2-1,3-benzoxadiazol-4-yl) (ammonium salt) (NBD-PE, 1 mol %), to avoid introducing steric interactions of the headgroup with the silica matrix. Figure 4 panels a and b show XRD patterns of lipid films before and after exposure to TMOS precursors at 37 °C. The patterns reflect the lamellar structure with a strong (001) diffraction peak at 50 Å for the control lipid assembly

TABLE 1. Phospholipid Phase Obtained for Various Spin-Coated Lipids upon Exposure to Silica Precursors. DMPC and egg PC Were Exposed to TEOS Precursor. POPC was exposed to TMOS Precursor[a]

lipid type	lipid	lipid tail composition chain length:no. of unsaturated bonds	structure (60 °C)
saturated	DMPC	14:0	lamellar
mixture	egg PC	16:0 (32.7%), 18:0 (12.3%), 18:1 (32%), 18:2 (17.1%), 20:4 (2.7%)	hexagonal
unsaturated	DOPC	18:1	hexagonal
saturated—unsaturated	POPC	16:0—18:1	lamellar (37 °C)

[a] For detailed structure and composition, please refer to Supporting Information, Figure SI 1.

(no silica) and 55 Å for the hybrid lipid—silica film. Both the control and hybrid films exhibit higher order diffraction (002), (003), (004) peaks. A TEM micrograph of the surface region of a hybrid POPC-silica thin film after 1-h exposure to TMOS vapor clearly indicates a lamellar structure (Figure 4c). No XRD peaks were observed after calcination, which suggests a collapse of the structure upon removal of the lamellar phospholipid assembly. Sequential fluorescence images of the silica-coated POPC multilamellar assemblies are shown in Figure 4e. FRAP measurements indicate that phospholipids in these multilamellar ultrathin films are diffusively mobile ($D = 0.1 \pm 0.04\ \mu m^2/s$) when placed in aqueous solution. It is interesting to note that these assemblies did not crack in aqueous conditions, possibly due to the low synthesis temperature. Also, no delamination was observed after repeated rinsing. These results confirm that POPC lipid assemblies exposed to TMOS in mild conditions (*i.e.*, 37 °C, no HCl) result in stable, relatively fluid, highly ordered lamellar hybrid assemblies.

The previous experiments with POPC and TMOS were repeated at 60 °C. Similar to the DMPC results above, a lamellar to hexagonal transition was observed if the vapor exposure time exceeded 1 h; it may be that less time was necessary for the transition due to increased fluidity of the POPC chains. The lamellar hybrid lipid assemblies with 30 min TMOS exposure were fluid at room temperature. However, when placed in 100% RH, the films cracked significantly over macroscopic scales, indicating that the synthesis temperature dictates the stability of the hybrid assembly (*i.e.*, lower reaction temperatures prevent silica cracking) (Figure 4d).

We attempted to measure FRAP in multilamellar lipid assemblies without silica; however, the lipid multilayers immediately delaminated upon immersion into aqueous solution. Typically, the multilamellar silica assemblies maintain structural stability for at least 6 months in air at low humidity conditions. This was verified by XRD, as no change in *d* spacing is observed after several months of storage (Supporting Information, Figure SI 6). Upon immersion in water, the lipid assemblies were stable (maintained fluorescence and fluidity) and we did not observe peeling of films as shown in FRAP images (Figure 4).

CONCLUSIONS

In summary, we have demonstrated a simple synthesis of hybrid thin films that incorporate phospholipid bilayer assemblies with lamellar or hexagonal ordering into a robust matrix. These stable hybrid constructs are consequentially able to preserve vital structural aspects of naturally occurring multilamellar lipid assemblies and may therefore serve as effective models for structure—function studies of such assemblies or as components in new bioinspired materials or devices. Figure 5 and Table 1 summarize the effect of lipid composition, time of exposure, and synthesis temperature on the structure of lipid—silica assemblies described above. Our results indicate that saturated lipids retain lamellar structure at lower synthesis temperatures; whereas, more fluid lipid assemblies (*i.e.*, lipids with unsaturated fatty acids) shift to a hexagonal structure with longer exposure to silica precursor or elevated synthesis temperatures. In conclusion, we are able to easily fabricate tunable robust and fluid hybrid lipid—silica assemblies with various mesostructure features through minimal adjustments to the synthesis conditions. Our laboratories are currently optimizing reaction conditions for successful incorporation of relevant transmembrane peptides and proteins into the hybrid lipid—silica assemblies described here.

MATERIALS AND METHODS

Materials. DMPC (14:0), DOPC 18:1 (*cis*), (DOPE, 18:1), L-α-phosphatidylcholine (egg PC), POPC, and NBD-PE were purchased from Avanti Polar Lipids, Alabama. Tetraethylorthosilicate (TEOS), tetramethylorthosilicate (TMOS), and other common reagents were purchased from Sigma Aldrich, MO, and used without further purification.

Ultrathin Lipid Silica Films. Lipid multilayers were synthesized by spin-coating the desired lipid at a concentration of 10 mg/mL in chloroform on clean silicon wafers at 3000 rpm for 1 min unless otherwise specified. These lipid coated silicon wafers were placed in a sealed chamber and exposed to vapors of a silica precursor (TEOS or TMOS, 2 mL) and HCl (0.1 N aq) for a period of 2 h at 60 °C, unless otherwise specified. The samples were carefully taken from the chamber and stored in the dark at room temperature.

Characterization. The films were characterized using XRD on a Scintag PAD V diffractometer with Cu Kα radiation (λ =1.5406 Å) in is $\theta-2\theta$ ($2\theta = 0.8°-10.0°$) step-scan mode using a 0.02° step size for 3 s. Analysis of the patterns was performed using MDI's Jade 9 software. TEM was performed on a JEOL 2010 equipped with a Gatan slow scan CCD camera at a 200 kV accelerating voltage. The samples were prepared either transferring a lipid film from a silicon substrate to a TEM grid using a surgical blade

or by using standard cross-section techniques. Calcination of samples was performed at 400 °C (heating rate of 1 °C per minute) for 4 h in air.

Fluorescence Recovery after Photobleaching. Lipid−silica assemblies were synthesized using a mixture of lipid POPC (10 mg/mL in chloroform) with tail labeled fluorescent 1 mol % NBD-PE. The resulting lipid solution was spin coated onto clean silicon wafers at 3000 rpm for 1 min. These lipid coated silicon wafers were placed in a sealed chamber and exposed to vapors of TMOS (2 mL) and water (2 mL) for a period of 1 h at 37 °C. The samples were carefully taken from the chamber and stored in the dark at room temperature. FRAP measurements were performed on a Zeiss LSM 510 Meta confocal scanning laser microscope equipped with an argon ion laser. As-synthesized samples were stored in the dark for 2 days followed by incubation in water for 2 h to determine the stability of the multilayers. Repeated scanning (512 times) of the laser resulted in bleaching the dye in the lipid layers. The 488 nm line of the Ar-ion laser was used for both bleaching and excitation of the fluorescent labeled lipids. The bleached samples were imaged after intervals of time sufficient to allow diffusive recovery. There was no detectable photobleaching during the recording of successive image scans.

Conflict of Interest: The authors declare no competing financial interest.

Acknowledgment. We gratefully acknowledge funding provided for this work by the National Science Foundation through the Research Triangle MRSEC (DMR-1121107), the Army Research Office (W911NF-06-1-0333), Center for Integrated Nanotechnologies (CINT), LANL, and the Department of Energy through the LANL/LDRD Program. We are grateful to Dr. A. Keilbach, Anton Paar, for performance of GISAXS measurements.

Supporting Information Available: An electronic file is available that contains Supporting Information including (i) structural information on the lipids used, (ii) XRD and TEM data on various lipid−silica assemblies, and (iii) procedure and results for GISAXS measurements. This material is available free of charge *via* the Internet at http://pubs.acs.org.

REFERENCES AND NOTES

1. Nagle, J. F.; Tristram-Nagle, S. Structure of Lipid Bilayers. *Biochim. Biophys. Acta* **2000**, *1469*, 159–195.
2. Higgins, C. F. ABC Transporters—from Microrganisms to Man. *Annu. Rev. Cell Biol.* **1992**, *8*, 67–113.
3. Benz, R.; Janko, K.; Lauger, P. Ionic Selectivity of Pores Formed by the Matrix Protein (Porin) of *Escherichia coli*. *Biochim. Biophys. Acta* **1979**, *551*, 238–247.
4. Szoka, F.; Papahadjopoulos, D. Comparative Properties and Methods of Preparation of Lipid Vesicles (Liposomes). *Annu. Rev. Biophys. Bioeng.* **1980**, *9*, 467–508.
5. Groves, J. T.; Ulman, N.; Boxer, S. G. Micropatterning Fluid Lipid Bilayers on Solid Supports. *Science* **1997**, *275*, 651–653.
6. Wagner, M. L.; Tamm, L. K. Tethered Polymer-Supported Planar Lipid Bilayers for Reconstitution of Integral Membrane Proteins: Silane-Polyethyleneglycol-Lipid as a Cushion and Covalent Linker. *Biophys. J.* **2000**, *79*, 1400–1414.
7. Holden, M. A.; Jung, S. Y.; Yang, T. L.; Castellana, E. T.; Cremer, P. S. Creating Fluid and Air-Stable Solid Supported Lipid Bilayers. *J. Am. Chem. Soc.* **2004**, *126*, 6512–6513.
8. Castellana, E. T.; Cremer, P. S. Solid Supported Lipid Bilayers: From Biophysical Studies to Sensor Design. *Surf. Sci. Rep* **2006**, *61*, 429–444.
9. De Felici, M.; Felici, R.; Ferrero, C.; Tartari, A.; Gambaccini, M.; Finet, S. Structural Characterization of the Human Cerebral Myelin Sheath by Small Angle X-ray Scattering. *Phys. Med. Biol.* **2008**, *53*, 5675–5688.
10. Haas, H.; Torrielli, M.; Steitz, R.; Cavatorta, P.; Sorbi, R.; Fasano, A.; Riccio, P.; Gliozzi, A. Myelin Model Membranes on Solid Substrates. *Thin Solid Films* **1998**, *327*, 627–631.
11. Stratton, C. J. Ultrastructure of Multilamellar Bodies and Surfactant in Human Lung. *Cell Tissue Res* **1978**, *193*, 219–229.
12. Petrache, H. I.; Dodd, S. W.; Brown, M. F Area Per Lipid and Acyl Length Distributions in Fluid Phosphatidylcholines Determined by H-2 NMR Spectroscopy. *Biophys. J.* **2000**, *79*, 3172–3192.
13. Nagle, J. F.; Zhang, R. T.; TristramNagle, S.; Sun, W. J.; Petrache, H. I.; Suter, R. M. X-ray Structure Determination of Fully Hydrated L(Alpha) Phase Dipalmitoylphosphatidylcholine Bilayers. *Biophys. J.* **1996**, *70*, 1419–1431.
14. Salditt, T.; Li, C.; Spaar, A.; Mennicke, U. X-ray Reflectivity of Solid-Supported, Multilamellar Membranes. *Eur. Phys. J. E* **2002**, *7*, 105–116.
15. Fragneto-Cusani, G. Neutron Reflectivity at the Solid/Liquid Interface: Examples of Applications in Biophysics. *J. Phys.: Condens. Matter* **2001**, *13*, 4973–4989.
16. Munster, C.; Salditt, T.; Vogel, M.; Siebrecht, R.; Peisl, J. Nonspecular Neutron Scattering from Highly Aligned Phospholipid Membranes. *Europhys. Lett.* **1999**, *46*, 486–492.
17. Perino-Gallice, L.; Fragneto, G.; Mennicke, U.; Salditt, T.; Rieutord, F. Dewetting of Solid-Supported Multilamellar Lipid Layers. *Eur. Phys. J. E* **2002**, *8*, 275–282.
18. Simonsen, A. C.; Bagatolli, L. A. Structure of Spin-Coated Lipid Films and Domain Formation in Supported Membranes Formed by Hydration. *Langmuir* **2004**, *20*, 9720–9728.
19. Harper, J. C.; Khirpin, C. Y.; Carnes, E. C.; Ashley, C. E.; Lopez, D. M.; Savage, T.; Jones, H. D. T.; Davis, R. W.; Nunez, D. E.; Brinker, L. M.; *et al.* Cell-Directed Integration into Three-Dimensional Lipid−Silica Nanostructured Matrices. *ACS Nano* **2010**, *4*, 5539–5550.
20. Besanger, T.; Zhang, Y.; Brennan, J. D. Characterization of Fluorescent Phospholipid Liposomes Entrapped in Sol−Gel Derived Silica. *J. Phys. Chem. B* **2002**, *106*, 10535–10542.
21. Gupta, G.; Rathod, S. B.; Staggs, K. W.; Ista, L. K.; Oucherif, K. A.; Atanassov, P. B.; Tartis, M. S.; Montano, G. A.; Lopez, G. P. CVD for the Facile Synthesis of Hybrid Nanobiomaterials Integrating Functional Supramolecular Assemblies. *Langmuir* **2009**, *25*, 13322–13327.
22. Avnir, D.; Coradin, T.; Lev, O.; Livage, J. Recent Bio-Applications of Sol-Gel Materials. *J. Mater. Chem.* **2006**, *16*, 1013–1030.
23. Nassif, N.; Bouvet, O.; Rager, M. N.; Roux, C.; Coradin, T.; Livage, J. Living Bacteria in Silica Gels. *Nat. Mater.* **2002**, *1*, 42–44.
24. Bagshaw, S. A.; Prouzet, E.; Pinnavaia, T. J. Templating of Mesoporous Molecular-Sieves by Nonionic Polyethyleneoxide Surfactants. *Science* **1995**, *269*, 1242–1244.
25. Beck, J. S.; Vartuli, J. C.; Roth, W. J.; Leonowicz, M. E.; Kresge, C. T.; Schmitt, K. D.; Chu, C. T. W.; Olson, D. H.; Sheppard, E. W.; McCullen, S. B.; *et al.* A New Family of Mesoporous Molecular-Sieves Prepared with Liquid Crystal Templates. *J. Am. Chem. Soc.* **1992**, *114*, 10834–10843.
26. Brinker, C. J.; Lu, Y. F.; Sellinger, A.; Fan, H. Y. Evaporation-Induced Self-Assembly: Nanostructures Made Easy. *Adv. Mater.* **1999**, *11*, 579–585.
27. Huo, Q. S.; Margolese, D. I.; Stucky, G. D. Surfactant Control of Phases in the Synthesis of Mesoporous Silica-Based Materials. *Chem. Mater.* **1996**, *8*, 1147–1160.
28. Nishiyama, N.; Tanaka, S.; Egashira, Y.; Oku, Y.; Ueyama, K. Vapor-Phase Synthesis of Mesoporous Silica Thin Films. *Chem. Mater.* **2003**, *15*, 1006–1011.
29. Tanaka, S.; Nishiyama, N.; Oku, Y.; Egashira, Y.; Ueyama, K. Nano-Architectural Silica Thin Films with Two-Dimensionally Connected Cagelike Pores Synthesized from Vapor Phase. *J. Am. Chem. Soc.* **2004**, *126*, 4854–4858.
30. Gupta, G.; Atanassov, P.; Lopez, G. P. Robust Hybrid Thin Films That Incorporate Lamellar Phospholipid Bilayer Assemblies and Transmembrane Proteins. *Biointerphases* **2006**, *1*, 6–10.
31. Luckarift, H. R.; Sizemore, S. R.; Roy, J.; Lau, C.; Gupta, G.; Atanassov, P.; Johnson, G. R. Standardized Microbial Fuel Cell Anodes of Silica-Immobilized Shewanella Oneidensis. *Chem. Commun.* **2010**, *46*, 6048–6050.
32. Duque, J. G.; Gupta, G.; Cognet, L.; Lounis, B.; Doorn, S. K.; Dattelbaum, A. M. New Route to Fluorescent Single-Walled Carbon Nanotube/Silica Nanocomposites: Balancing Fluorescence Intensity and Environmental Sensitivity. *J. Phys. Chem. C* **2011**, *115*, 15147–15153.

33. Duque, J. G.; Hamilton, C. E.; Gupta, G.; Crooker, S. A.; Crochet, J. J.; Mohite, A.; Htoon, H.; Obrey, K. A. D.; Dattelbaum, A. M.; Doorn, S. K. Fluorescent Single-Walled Carbon Nanotube Aerogels in Surfactant-Free Environments. *ACS Nano* **2011**, *5*, 6686–6694.
34. Albertorio, F.; Diaz, A. J.; Yang, T. L.; Chapa, V. A.; Kataoka, S.; Castellana, E. T.; Cremer, P. S. Fluid and Air-Stable Lipopolymer Membranes for Biosensor Applications. *Langmuir* **2005**, *21*, 7476–7482.
35. Deng, Y.; Wang, Y.; Holtz, B.; Li, J. Y.; Traaseth, N.; Veglia, G.; Stottrup, B. J.; Elde, R.; Pei, D. Q.; Guo, A.; *et al*. Fluidic and Air-Stable Supported Lipid Bilayer and Cell-Mimicking Microarrays. *J. Am. Chem. Soc.* **2008**, *130*, 6267–6271.